Energy Management Strategies for Vehicular Electric Power Systems

Michiel Koot, J. T. B. A. Kessels, *Student Member, IEEE*, Bram de Jager, W. P. M. H. Heemels, P. P. J. van den Bosch, *Member, IEEE*, and Maarten Steinbuch, *Senior Member, IEEE*

***Abstract*—In the near future, a significant increase in electric power consumption in vehicles is expected. To limit the associated increase in fuel consumption and exhaust emissions, smart strategies for the generation, storage/retrieval, distribution, and consumption of electric power will be used. Inspired by the research on energy management for hybrid electric vehicles (HEVs), this paper presents an extensive study on controlling the vehicular electric power system to reduce the fuel use and emissions, by generating and storing electrical energy only at the most suitable moments. For this purpose, both off-line optimization methods using knowledge of the driving pattern and on-line implementable ones are developed and tested in a simulation environment. Results show a reduction in fuel use of 2%, even without a prediction of the driving cycle being used. Simultaneously, even larger reductions of the emissions are obtained. The strategies can also be applied to a mild HEV with an integrated starter alternator (ISA), without modifications, or to other types of HEVs with slight changes in the formulation.**

***Index Terms*—Energy management, fuel reduction, hybrid electric vehicles (HEVs), regenerative braking, vehicular electric power system.**

I. Introduction

THE electric power consumption in standard road vehicles has increased significantly over the past twenty years (approximately four percent every year) and in the near future even higher power demands are expected [1]–[3]. Reasons for this trend are as follows:

- Today's customers expect more performance, comfort, and safety from new vehicles;
- Electrical devices replace mechanical or hydraulic components in the vehicle (e.g., the drive-by-wire concept).

To keep up with future power demands, the automobile industry has suggested new 42-V power net topologies which should extend (or replace) the traditional 14-V power net from present vehicles [1]–[5]. Although these advanced power nets will be able to meet tomorrow's power requirements, a problem that arises is how to control the power net, in order to obtain maximum energy efficiency within the vehicle. One way is to improve the efficiency of the electric components [6]. In addition, energy management can be used.

In a conventional vehicle, the alternator tries to maintain a fixed voltage level on the power net. A traditional lead-acid battery is present for supplying key-off loads and for making the power net more robust against peak-power demands. Although the battery offers freedom to the alternator in deciding when to generate power, this freedom is generally not used.

The research described in this paper exploits this freedom as it replaces the conventional alternator with an advanced alternator that is power controlled. The alternator is directly coupled to the engine's crankshaft, so by controlling its output power, it will influence the operating point of the combustion engine, and thus the fuel use of the vehicle. Several control strategies will be presented that control the alternator such that it generates the required amount of electric energy in a more beneficial way by temporarily charging and discharging the battery.

In Fig. 1, it is shown how the energy management controller interacts with the vehicle. Based on information of the current vehicle state and possibly prediction of the future vehicle state, the electric power setpoint is provided to the alternator and a feed forward torque compensation is given to the engine.

In recent years, a lot of research is carried out in the field of hybrid electric vehicles (HEV). Especially the research activities on energy management in a parallel HEV (see, e.g., [7] for an overview) address many useful concepts that are strongly related to the research shown here.

In a parallel HEV, an electric machine accompanies the internal combustion engine (ICE), in order to provide tractive force to the drive train. Moreover, the electric machine can operate in alternator mode for converting mechanical power into electric power. The alternator mode is similar to a vehicle with a conventional power train but with an advanced power net. Although the electric power requirements in a parallel HEV are higher than in a conventional vehicle with a 42-V power net, both configurations could use the same concepts for controlling the generation of electric power.

Because of the relevance to the work presented in this paper, a short overview will be given on control methods in energy management strategies for HEV. Strategies that are based on heuristics can be easily implemented in a real vehicle by using a rule-based strategy [8] or by using fuzzy logic [9]. Although these strategies can offer a significant improvement in energy efficiency, it is clear that they do not guarantee an optimal result

Manuscript received October 7, 2004; revised January 2, 2005 and January 30, 2005. The review of this paper was coordinated by Prof. A. Emadi.

M. Koot, B. de Jager, and M. Steinbuch are with the Dynamics and Control Technology Group, Department of Mechanical Engineering, Technische Universiteit Eindhoven, 5600 MB Eindhoven, The Netherlands (e-mail: M.W.T.Koot@tue.nl; A.G.de.Jager@wfw.wtb.tue.nl; M.Steinbuch@tue.nl).

J. T. B. A. Kessels and P. P. J. van den Bosch are with the Control Systems Group, Department of Electrical Engineering, Technische Universiteit Eindhoven, 5600 MB Eindhoven, The Netherlands (e-mail: J.T.B.A.Kessels@tue.nl; P.P.J.v.d.Bosch@tue.nl).

W. P. M. H. Heemels is with the Embedded Systems Institute, 5600 MB Eindhoven, The Netherlands (e-mail: Maurice.Heemels@embeddedsystems.nl).

Digital Object Identifier 10.1109/TVT.2005.847211

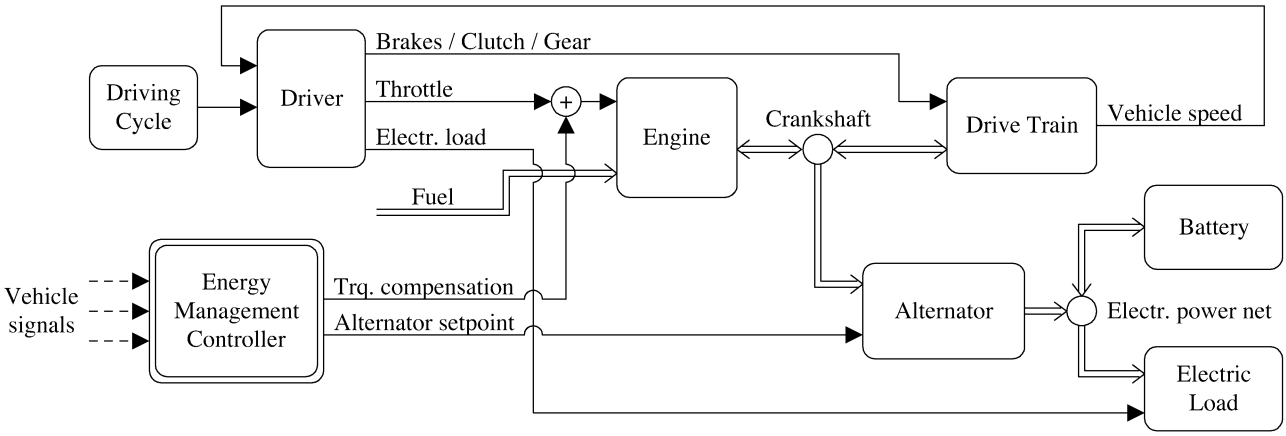

Fig. 1. Energy management controller in the vehicle.

in all situations. Consequently, strategies emerged that are based on optimization techniques.

To find the global optimal solution, control techniques such as linear programming [10], optimal control [11], and especially dynamic programming (DP) [12]–[15] have been studied. In general, these techniques do not offer an on-line solution, because they assume that the future driving cycle is entirely known. Nevertheless, their result can be used as a benchmark for the performance of other strategies, or to derive rules for a rule-based strategy. If only the present state of the vehicle is considered, optimization of the operating points of the individual components can still be beneficial, but profits will be limited, see [16]–[18].

A different approach is taken in [19], [20]. Instead of considering one particular driving cycle, a certain set of driving cycles is considered, resulting in a stochastic optimization approach. A difficulty will be to cover a real-world driving situation with a set of individual driving cycles. Promising results on the prediction of the vehicle load in the near future make it possible to execute the optimization over a short horizon [15]. In this case, the benefits of a control strategy are directly related to the accuracy of the prediction information. One step further is to incorporate the optimization into a Model Predictive Control (MPC) framework [12], such that the energy management strategy will be able to anticipate on upcoming events. Again, the quality of the prediction information as well as the length of the prediction horizon determine the success of the control strategy.

After considering the optimization based methods developed for HEVs, this paper presents a practically implementable strategy that is directly derived from global optimization methods, thereby continuing on the approach of [21]–[23].

After modeling and analyzing the relevant components of the vehicle, we start with a formal problem definition, by expressing the total fuel consumption and emissions along the driving cycle as a function of the control variables.

To find the optimal control sequence for the alternator, DP has been applied. Under the assumption that the entire driving cycle is known in advance, the method calculates the power setpoints for the alternator. For the problem formulation considered here, several modifications of the algorithm are carried out, thereby reducing the amount of computations. Nevertheless, the computation time of DP still remains too large for a practical real-world application.

To come to a solution that is implementable in a vehicle, additional modifications are necessary, as follows. First, the vehicle model is further simplified, such that the problem formulation reduces to a simpler quadratic programming (QP) structure. However, this solution still depends on the assumption that information about the driving cycle in the near future is available. Second, based on the QP formulation, a strategy is designed that only requires vehicle information from the past and the present.

The remainder of this paper is built up as follows: The vehicle will be modeled in Section II. Section III formulates the energy management problem as an optimization problem. The DP strategy is explained in Section IV. Section V reduces the problem to a QP problem. Section VI presents an on-line implementable strategy. The performances of all individual strategies are compared by simulations in Section VII. Section VIII discusses how the strategies carry over to HEVs. Conclusions are given in Section IX.

II. Vehicle Model

The type of vehicles considered in this paper are vehicles with a conventional drive train and a manual transmission. In Fig. 2 the structure of such a vehicle is represented as a power-based model. The drive train block contains all drive train components including clutch, gears, wheels, and inertia. The alternator is connected to the engine with a fixed gear ratio.

The power flow in the vehicle starts with fuel that goes into the internal combustion engine. The mechanical power that comes out of the engine splits up into two directions: one part goes to the mechanical drive train for vehicle propulsion, whereas the other part goes to the alternator. The alternator provides electric power for the electric loads but also takes care of charging the battery. In the end, the power becomes available for vehicle propulsion and for electric loads connected to the power net.

The power flow through the battery can be positive as well as negative. If an integrated starter alternator (ISA) is used, the alternator power can also be negative.

The goal of the energy management system as considered in this paper is to control the alternator power such that the fuel

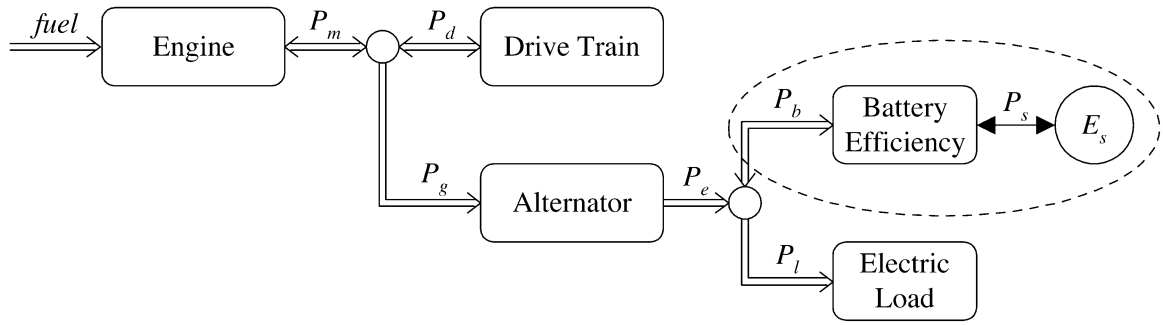

Fig. 2. Power flow in the vehicle.

consumption and emissions are reduced, while the drivability remains unaffected, i.e., the driver should not experience different vehicle behavior when the controller is applied. This requirement greatly reduces the problem complexity. It implies that the vehicle speed and thus the drive train torque and engine speed remain unaffected and therefore it is possible to use them as given information.

The remaining components of interest are the engine, the alternator, and the battery. Using discrete time optimization with a sampling interval of 1 s or larger, the dynamic behavior of the engine and the alternator can be neglected, so their characteristics are represented by static models. The only remaining dynamics in the model is the integrator of the battery storage.

A. Engine

The internal combustion engine is represented by a nonlinear static map which describes the relation between fuel consumption, engine speed, and engine power

$$\text{fuelrate} = f(P_m, \omega) \quad \text{where} \quad P_m = P_d + P_g. \tag{1}$$

Here P_m is the mechanical power delivered by the engine, P_d is the part needed for propulsion, P_g goes to the alternator, while ω is the engine crank speed. Note that the engine torque can be derived from the engine power if the engine speed is known.

A characteristic fuel map of a spark ignition engine is displayed in Fig. 3, where fuel rate curves $f(P_m, \omega)$ are drawn for different engine speeds ω as function of engine power P_m.

The exhaust emissions of CO_2, CO, NO_x, and HC (hydrocarbons) are also represented by a static map, although they are more influenced by dynamic and temperature effects than the fuel use.

B. Alternator

Using a similar approach, the alternator model reduces to a static nonlinear map

$$P_g = g(P_e, \omega) \quad \text{where} \quad P_e = P_l + P_b. \tag{2}$$

Here P_e is the electric power delivered by the alternator, P_l is the electric load, and P_b is the power going into or out of the battery.

C. Battery

The battery characteristic is modeled by

$$P_b = P_s + P_{\text{loss}}(P_s, E_s, T). \tag{3}$$

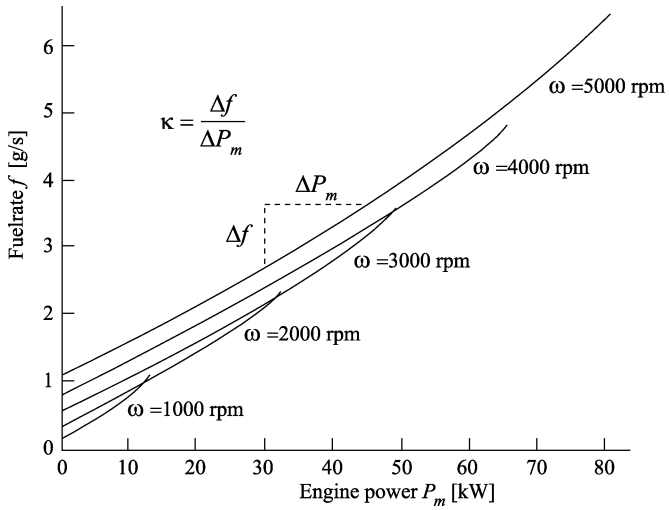

Fig. 3. Characteristic fuel map of an engine.

P_s represents the power actually stored in the battery, P_{loss} represents the battery losses that depend on the storage power P_s, the energy level in the battery E_s, and the temperature T. A typical static charge/discharge power storage curve is shown in Fig. 4.

The losses in the battery are positive for both charging and discharging. This can be obtained by modeling the losses quadratic with the storage power

$$P_b \approx P_s + \beta P_s^2. \tag{4}$$

For simplicity, the influence of E_s and T, and differences between charging and discharging are neglected here.

The battery energy level is given by a simple integrator

$$E_s(t) = E_s(0) + \int_0^t P_s(\tau)\mathrm{d}\tau. \tag{5}$$

The state of charge (SOC) is the relative energy level

$$\text{SOC} = \frac{E_s}{E_{\text{cap}}} \cdot 100\% \tag{6}$$

where E_{cap} is the energy capacity of the battery.

III. Problem Definition

The idea of controlling the alternator power is initiated by the fact that energy losses in the internal combustion engine, alternator, and battery change according to their operating point.

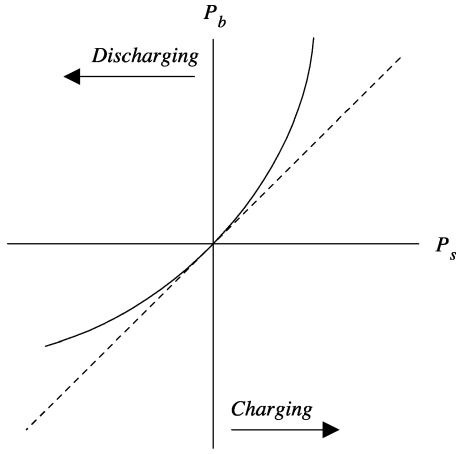

Fig. 4. Battery power map.

Minimizing these energy losses will result in an energy management strategy achieving higher fuel economy.

To explain the basic idea behind this control strategy, consider, for convenience, the fuel map given in Fig. 3, although the actual strategy also involves the alternator and battery characteristics and the emission maps.

As driver requests have to be fulfilled, one cannot change the power to the drive train P_d nor the engine speed ω assuming manual gearshifts. However, the storage capacity of the battery allows changes in the alternator's setpoint while still all electric load requests are fulfilled. It is clear that such control actions introduce freedom in shifting the operating point of the engine to other regions. Intuitively, one can find profitable control actions for the alternator by considering the gradient of the fuel map curves, the so-called *incremental fuel rate* κ

$$\kappa = \frac{\Delta f}{\Delta P_m}. \tag{7}$$

At points where κ is small, it is relatively cheap to generate electric energy. This energy will be stored in the battery and can be used at moments when it is less profitable (i.e., κ large) to activate the alternator. To yield a positive effect on the total fuel economy of the vehicle, energy losses in the battery must be smaller than the profits obtained in the fuel map.

A. Control Objective and Constraints

The control objective of energy management is to lower the fuel consumption and exhaust emissions while satisfying several constraints. This control problem can be formulated as an optimization problem

$$\min_{\underline{x}} J(\underline{x}) \quad \text{subject to} \quad G(\underline{x}) \leq 0. \tag{8}$$

Assuming the signals $\omega(t)$, $P_d(t)$, and $P_l(t)$ to be known, and combining the characteristics of all components, given by (1), (2), and (4), the fuel rate can be expressed as a function of the battery storage power

$$\text{fuelrate}(\omega, P_d, P_l, P_s) = \text{fuelrate}(P_s). \tag{9}$$

The cost function expresses the fuel use over the driving cycle in the time interval $[0, t_e]$

$$J = \text{fuel}(P_s) = \int_0^{t_e} \text{fuelrate}(P_s)\mathrm{d}t. \tag{10}$$

Although P_s represents the design variable $\underline{x}$, the actual controlled input is P_e. Because the relation between P_s and P_e is known, P_e can be computed from the optimal P_s.

Instead of minimizing the fuel use only, the cost function can also be a weighted sum of the fuel use and the exhaust emissions by using

$$\begin{aligned}\gamma(P_s) = {} & w_1 \text{fuelrate}\,(P_s) + w_2 CO_2(P_s) \\ & + w_3 CO(P_s) + w_4 NO_x(P_s) + w_5 HC(P_s)\end{aligned} \tag{11}$$

where w_i are weighting factors.

The operating range of the components is limited, so bounds have to be set on the engine power, electrical power, and battery power throughput. This can be done using the following constraints

$$P_{m\,\min} \leq P_m \leq P_{m\,\max} \tag{12}$$

$$P_{e\,\min} \leq P_e \leq P_{e\,\max} \tag{13}$$

$$P_{b\,\min} \leq P_b \leq P_{b\,\max}. \tag{14}$$

Because the relations (2) and (4) are invertible, the constraints (12)–(14) can be translated to time varying bounds on P_s. Combining them leads to one lower and upper bound for P_s at each time instant

$$P_{s\,\min} \leq P_s \leq P_{s\,\max}. \tag{15}$$

Using (5), the bounds on the battery energy level can be translated to constraints on P_s

$$E_{s\,\min} - E_s(0) \leq \int_0^t P_s(\tau)\mathrm{d}\tau \leq E_{s\,\max} - E_s(0). \tag{16}$$

A charge-sustaining vehicle requires some kind of endpoint penalty to guarantee that the state of charge of the battery remains in a neighborhood around a desired value. An endpoint constraint will be used here, requiring the state of charge at the end of the cycle to be the same as at the beginning

$$E_s(t_e) = E_s(0) \Rightarrow \int_0^{t_e} P_s(t)\mathrm{d}t = 0. \tag{17}$$

B. Applied Control Techniques

The nonlinear optimization problem can be carried out using nonlinear problem solvers. The problem is defined such that it can be easily incorporated into an optimization technique called Dynamic Programming (DP) [24], as will be done in Section IV.

Because computation time is limited in on-line applications, the nonlinear optimization problem will be approximated by a Quadratic Programming (QP) [25] problem in Section V. For

practical data, the problem is convex, which makes solution easier.

In reality, only a limited prediction of the future driving cycle will be available. A possible control technique that is able to use this prediction is Model Predictive Control (MPC) [26], which will be the topic of Section VI.

IV. Dynamic Programming

After discretization, the optimization problem formulated in the previous section can be seen as a multistep decision problem: at each time instant, one has to decide which alternator setpoint, for the next time interval, will achieve the smallest objective value over a certain trajectory, while satisfying the constraints. To find this optimal control sequence, DP [24] will be applied.

DP is commonly used for global optimization of the energy management problem of HEVs [12]–[15]. For the problem formulation considered here, several modifications can be carried out, thereby reducing the amount of computations.

A. Implementation DP Algorithm

Equations (1), (2), (4), and (5) define the fuel consumption of a dynamic system with one control input P_s and one state variable E_s. To keep track of the energy level in the battery, a discrete version of (5) is used

$$E_s(k) = E_s(k-1) + P_s(k)\Delta t. \tag{18}$$

Note that the sample time Δt is fixed, whereas signals are kept constant in between. The sample moments are indicated by variable $k = [1, \ldots, n]$ with n defined by the length of the driving cycle

$$n = \left\lceil \frac{t_e}{\Delta t} \right\rceil. \tag{19}$$

Due to the bounds (16), only energy levels between $E_{s\,\min}$ and $E_{s\,\max}$ will be used. This area is mapped onto a fixed grid with distance ΔE_s, such that exactly $m+1$ energy levels are considered, with

$$m = \left\lfloor \frac{E_{s\,\max} - E_{s\,\min}}{\Delta E_s} \right\rfloor. \tag{20}$$

The relation between the input variable P_s and the state E_s is an integrator. As will be explained at the end of this section, it is computationally beneficial to select a grid for P_s that is directly related to ΔE_s. Therefore, ΔP_s is chosen as

$$\Delta P_s = \frac{\Delta E_s}{\Delta t}. \tag{21}$$

The control input P_s should respect the constraint (15). It will be selected from a discrete set of input values, separated with grid distance ΔP_s. The set of feasible input grid points at each time instant k can be defined as

$$\mathcal{P}_s(k) = \{u | u \in \mathbb{N}, \quad P_{s\,\min}(k) \le u(k)\Delta P_s \le P_{s\,\max}(k)\}. \tag{22}$$

The operating range of the battery reduces further by considering only those trajectories that are possible between an initial energy level of the battery $E_s(0)$ and a desired end state $E_s(n)$. For convenience, both $E_s(0)$ and $E_s(n)$ are restricted to one of the grid points for E_s. Consequently, both energy levels can be represented by an integer $e \in [0, \ldots, m]$

$$\text{Initial energy level } e_0 : E_s(0) = E_{s\,\min} + e_0 \Delta E_s$$
$$\text{Final energy level } e_n : E_s(n) = E_{s\,\min} + e_n \Delta E_s.$$

Due to the endpoint constraint (17), $e_n = e_0$ holds.

The feasible area for E_s along the driving cycle is restricted by six individual constraints, i.e., the upper and lower bound on P_s, the upper and lower bound on E_s, the initial state $E_s(0)$, and the end state $E_s(n)$. Together, they define stricter boundaries on E_s, given by

$$E^*_{s\,\min} = \max\left(\mathrm{E}_{\mathrm{s\ min}}, \mathrm{E}^1_{\mathrm{s\ min}}, \mathrm{E}^2_{\mathrm{s\ min}}\right) \tag{23}$$
$$E^*_{s\,\max} = \min\left(\mathrm{E}_{\mathrm{s\ max}}, \mathrm{E}^1_{\mathrm{s\ max}}, \mathrm{E}^2_{\mathrm{s\ max}}\right) \tag{24}$$

where

$$E^1_{s\,\min}(k) = E_s(0) + \sum_{i=1}^{k} P_{s\,\min}(i)\Delta t \tag{25}$$
$$E^2_{s\,\min}(k) = E_s(n) - \sum_{i=k+1}^{n} P_{s\,\max}(i)\Delta t \tag{26}$$
$$E^1_{s\,\max}(k) = E_s(0) + \sum_{i=1}^{k} P_{s\,\max}(i)\Delta t \tag{27}$$
$$E^2_{s\,\max}(k) = E_s(n) - \sum_{i=k+1}^{n} P_{s\,\min}(i)\Delta t. \tag{28}$$

These boundaries are illustrated in Fig. 5. Typically, the feasible area has a diamond-shape. Starting from an initial state $E_s(0)$, it is possible to charge or discharge the battery until one of the boundaries $E_{s\,\max}$ or $E_{s\,\min}$ becomes active. It is allowed to stay between those boundaries, as long as the end of the driving cycle is sufficiently far away. In the end, it is necessary to return to $E_s(n)$, so the feasible area of E_s converges according to the limitations on P_s.

The energy levels e that are feasible are different at each time instant. Given the boundaries (23) and (24), it is possible to define a set $\mathcal{R}$ that represents all feasible combinations (e,k) for a given driving cycle

$$\mathcal{R} = \{(e,k) | 0 \le e \le m,\ 1 \le k \le n, \\ E^*_{s\,\min}(k) \le E_{s\,\min} + e\Delta E_s \le E^*_{s\,\max}(k)\}. \tag{29}$$

The DP algorithm creates a cost matrix $\mathbf{R} \in \mathbb{R}^{(m+1)\times n}$ and fills this matrix recursively from $k = n$ down to $k = 1$. In literature, $\mathbf{R}$ is often called the cost-to-go matrix. Here, it represents the amount of fuel and emissions necessary to reach the end of the driving cycle

$$\mathbf{R}_{e,k} = \text{the minimum cumulative cost for driving the remainder of the driving cycle, starting at } t = k\Delta t \text{ with an initial state } E_s(k) = E_{s\,\min} + e\Delta E_s.$$

Using (22) and (29), it is possible to formulate a recursive definition for matrix $\mathbf{R}$. The DP algorithm uses the following expressions to calculate the contents of $\mathbf{R}$

$$\mathbf{R}_{e_n,n} = 0 \tag{30}$$
$$\mathbf{R}_{e,k} = \min_u \left(\mathbf{R}_{e+u,k+1} + \gamma(u\Delta P_s, k)\Delta t\right) \tag{31}$$

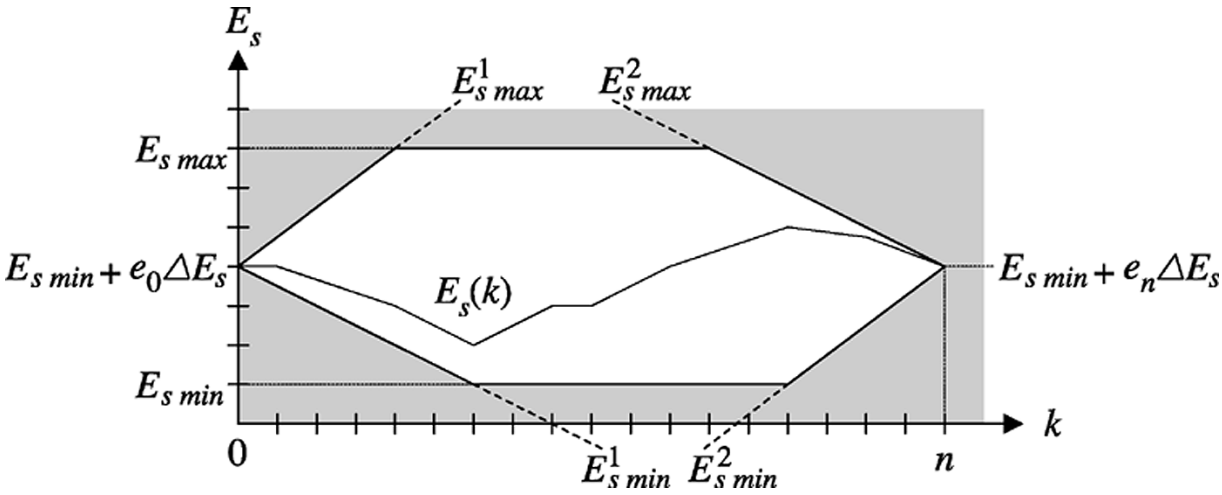

Fig. 5. Feasible energy window for battery along driving cycle.

for $k = [n-1, \ldots, 1]$, subject to

$$u \in \mathcal{P}_s(k) \tag{32}$$

$$(e, k) \in \mathcal{R} \tag{33}$$

$$(e+u, k+1) \in \mathcal{R}. \tag{34}$$

From (31) it should become clear why it is beneficial to select ΔE_s and ΔP_s according to (21). Consider the dynamics of the battery as described in (18). If the present state $E_s(k)$ is selected such that it corresponds exactly to one of the $m+1$ grid points, then the next state $E_s(k+1)$ will also be an energy level that matches exactly to a grid point, so there is no interpolation needed. This explains why the first term in (31) can be taken directly from cost matrix $\mathbf{R}$, without further calculations. Consequently, the calculation time of the DP-algorithm reduces significantly.

The sequence of P_s that achieves minimum fuel consumption is not stored in $\mathbf{R}$. The optimal values are calculated afterwards, by starting at $E_s(0)$ and then following the path of minimal cost, as it has been stored in $\mathbf{R}$. Given this sequence for $P_s(k)$, the requested setpoints for the alternator are found using (2) and (4).

All calculations required for DP can be done in an acceptable amount of time due to the simple dynamics (only the energy level in the battery) and all the restrictions on E_s and P_s. However, the number of computations increases rapidly with the driving cycle length and the grid density.

V. Quadratic Programming

Although the computation time of the DP routine has been reduced significantly, as discussed in Section IV, it is still very time consuming for long driving cycles, so for real-time implementation other modifications need to be considered. In this section, simplifications will be introduced to achieve a QP structure [25], which has the advantage that a global minimum is guaranteed and short computation times can be achieved, provided that the problem is convex. Limiting the prediction length of the driving cycle in the optimization is the subject of Section VI.

A QP problem is given by a quadratic cost criterion subject to linear constraints

$$\min_{\underline{x}} \frac{1}{2}\underline{x}^T H \underline{x} + \underline{h}^T \underline{x} + h_0 \quad \text{subject to} \quad A\underline{x} \leq \underline{b}. \tag{35}$$

A. Model Approximation

To obtain a quadratic cost function, the nonlinear relation for $\gamma(P_s)$ is approximated as a convex quadratic relation

$$\gamma(P_s) \approx \varphi_2 P_s^2 + \varphi_1 P_s + \varphi_0, \quad \varphi_2 > 0 \tag{36}$$

where parameters φ_i are time varying, as they depend on ω, P_d, and P_l. The approximation is done at each time instant, for the valid range of P_s, given by (15).

B. Cost Function

The cost function is the weighted sum of fuel use and emissions over the driving cycle. By discretization one may obtain

$$J = \sum_{k=1}^{n} \gamma\left(P_s(k)\right) \Delta t. \tag{37}$$

The sample time Δt may be omitted, since it is constant.

Returning to (35), this means that H is diagonal with

$$H(k,k) = 2\varphi_2(k). \tag{38}$$

The other terms become

$$\underline{h}(k) = \varphi_1(k) \quad \text{and} \quad h_0 = \sum_{k=1}^{n} \varphi_0(k). \tag{39}$$

The design variables are

$$\underline{x} = \underline{P}_s = [P_s(1), \ldots, P_s(n)]^T. \tag{40}$$

C. Constraints

The bounds on P_s (15), that include the bounds on P_m, P_e, and P_b are still present. The bounds on E_s can be written as linear constraints on P_s, by using the following discretization

$$E_s(k) = E_s(0) + \sum_{i=1}^{k} P_s(i)\Delta t. \tag{41}$$

The equality constraint (17) becomes

$$E_s(n) = E_s(0) \quad \Rightarrow \quad \sum_{k=1}^{n} P_s(k) = 0. \tag{42}$$

From (15), (41), and (42) it is easy to construct A and $\underline{b}$ in (35).

D. Solution

When only the upper and lower bounds on P_s and the equality constraint are taken into account, the exact solution of the problem can be solved efficiently with a routine described in [27]. If the upper and lower bound on E_s or other constraints are taken into account, a general QP solver must be used.

VI. Model Predictive Control

When the complete driving cycle is known *a priori*, the optimization problem has to be solved only once. However, if only a limited prediction horizon is available, both the DP and QP problem can be used within a MPC structure using a receding horizon [26].

This means that the optimization is carried out at each time step over a limited prediction horizon. The first value of the optimal control sequence is implemented. The next time step a new optimization is done using an updated prediction and new measurement data.

In [12], DP optimization is used within an MPC framework for a HEV. As shown in [22], for short prediction horizons, the variation in P_s and thus the performance is limited by the endpoint constraint on E_s. Inspired by [27], a new approach based on QP that does not rely on an accurate prediction has been developed.

A. Reduction of the QP Problem

If only the cost function and the equality constraint are considered, the QP problem can be solved analytically by introducing the Lagrange function

$$L(\underline{P}_s,\lambda)=\sum_{k=1}^{n}\left(\varphi_2(k)P_s(k)^2+\varphi_1(k)P_s(k)\right)-\lambda\sum_{k=1}^{n}P_s(k). \tag{43}$$

The optimal solution can be calculated by solving

$$\frac{\partial L(\underline{P}_s,\lambda)}{\partial \underline{P}_s}=0 \quad \text{and} \quad \frac{\partial L(\underline{P}_s,\lambda)}{\partial \lambda}=0. \tag{44}$$

The solution is given by

$$P_s^o(k)=\frac{\lambda-\varphi_1(k)}{2\varphi_2(k)} \tag{45}$$

where

$$\lambda=\frac{\sum_{k=1}^{n}\frac{\varphi_1(k)}{2\varphi_2(k)}}{\sum_{k=1}^{n}\frac{1}{2\varphi_2(k)}}. \tag{46}$$

This requires that $\varphi_2>0$, so the cost function J must be strictly convex.

The incremental costs are given by

$$\frac{\partial\gamma(P_s)}{\partial P_s}=2\varphi_2(k)P_s(k)+\varphi_1(k). \tag{47}$$

By substituting (45), it follows that the optimal solution is characterized by equal incremental cost, namely λ.

B. Elimination of the Prediction Horizon

Although for the computation of $P_s^o(k)$ only current values $\varphi_1(k)$ and $\varphi_2(k)$ are needed, computation of the value of λ requires knowledge of φ_1 and φ_2 over the entire driving cycle.

When a prediction of the complete cycle is not available, λ can be estimated or adapted on-line, for instance by using the following PI-type controller

$$\lambda(k+1)=\lambda_0+K_P(E_s(0)-E_s(k))+K_I\sum_{i=1}^{k}(E_s(0)-E_s(i))\,\Delta t \tag{48}$$

where λ_0 is an initial guess.

Because P_s is proportional with λ, and E_s is the integral of P_s, the closed loop becomes a discrete time version of a time varying second-order dynamic system

$$E_s(k+1)=E_s(k)+\frac{\Delta t}{2\varphi_2(k)}\cdot\Bigg\{\lambda_0-\varphi_1(k) +K_P\left(E_s(0)-E_s(k)\right)+K_I\sum_{i=1}^{k}\left(E_s(0)-E_s(i)\right)\Delta t\Bigg\}. \tag{49}$$

If the initial value λ_0 is chosen too high, the SOC will increase, which will lead to a lower value of λ. If λ_0 is chosen too low, the SOC will decrease, which will lead to a higher value of λ.

The feedback of E_s is meant to avoid draining or overcharging the battery in the long run, but short term fluctuations of E_s should still be possible, so the bandwidth of the PI-controller should be chosen rather low.

The use of feedback will add some robustness to the system. It is also possible to use MPC with zone control instead of the PI controller (48), such that λ is only adapted if the SOC exceeds some boundary, see [28].

For given λ, computing $P_s^o(k)$ using (45) is equivalent to solving at each time instant k

$$P_s^o(k)=\arg\min_{P_s(k)}\left\{\varphi_2(k)P_s(k)^2+\varphi_1(k)P_s(k) +\varphi_0(k)-\lambda P_s(k)\right\}. \tag{50}$$

Instead of the quadratic approximation, the original nonlinear cost function can also be used

$$P_s^o(k)=\arg\min_{P_s(k)}\left\{\gamma\left(P_s(k),k\right)-\lambda P_s(k)\right\}. \tag{51}$$

This can be solved using DP with a horizon length of 1 on a dense grid.

The bounds on P_s can be respected by saturation

$$P_s'(k)=\min\left(\max\left(P_{s\,\min}(k),P_s^o(k)\right),P_{s\,\max}(k)\right). \tag{52}$$

Equation (51) provides a nice physical interpretation of the control strategy. At each time instant the actual incremental cost for storing energy is compared with the average incremental cost. Energy is stored when generating now is more beneficial than average, whereas it is retrieved when it is less beneficial.

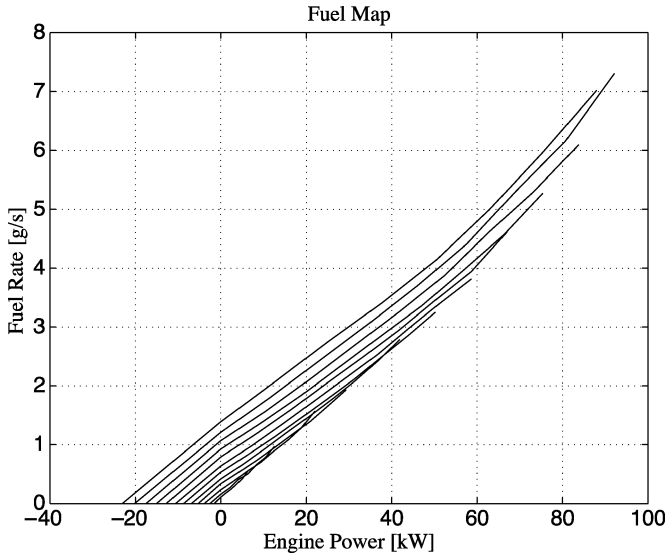

Fig. 6. Fuel map.

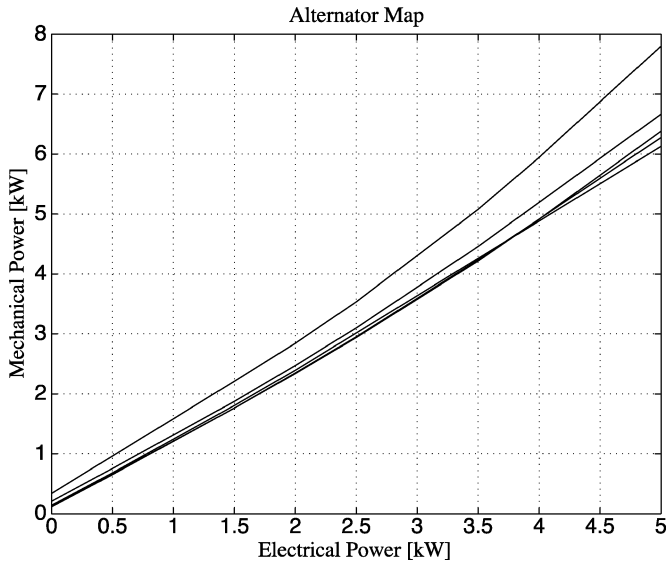

Fig. 7. Alternator map.

VII. Results

A. Simulation Model

Simulations are done for a conventional vehicle equipped with a 100-kW 2.0-L SI engine and a manual transmission with five gears. A 42-V 5-kW alternator and a 36-V 30-Ah lead-acid battery make up the alternator and storage components of the 42-V power net.

The fuel map and the alternator map are shown in Figs. 6 and 7, respectively.

The battery has an energy capacity of $E_{\text{cap}} = 4 \cdot 10^6$ J and is operated around 70% SOC, because the efficiencies for both charging and discharging in this range are acceptable. Parameter β of the battery model (4) has a value of $5 \cdot 10^{-5}$ W^{-1}, which gives an efficiency of 95% at 1000 W and 90% at 2000 W.

For a given speed profile and selected gears, the corresponding engine speed and torque needed for propulsion can be calculated using

$$\omega(t) = \frac{f_r}{w_r} g_r(t) v(t) \tag{53}$$

$$\tau_d(t) = \frac{w_r}{f_r} \frac{1}{g_r(t)} F_d(t) \tag{54}$$

$$F_d(t) = m\dot{v}(t) + \frac{1}{2}\rho C_d A_d v(t)^2 + mgC_r. \tag{55}$$

The parameters and their values are given in Table I.

When the engine speed drops below 700 rpm, the clutch is opened. The engine speed remains at an idle speed of 700 rpm and the engine power is equal to the alternator power. The drive train power becomes equal to the brake power.

When the drive train power is negative and the clutch is closed, the power is partly delivered by the internal combustion engine (which has a negative drag power), by the alternator, and by the brakes. Because regenerative braking delivers electrical power without extra fuel use, it is expected that it will be used as much as possible. The brakes are only used when the desired deceleration power is larger than the maximum negative power that can be taken up by the engine and the alternator.

TABLE I
Parameters of the Simulation Model

Quantity	*Symbol*	*Value*	*Unit*
Mass	m	1400	kg
Frontal area	A_d	2	m^2
Air drag coefficient	C_d	0.3	-
Rolling resistance	C_r	0.015	-
Air density	ρ	1.2	kg/m^3
Gravity	g	9.8	m/s^2
Wheel radius	w_r	0.3	m
Final drive ratio	f_r	4.0	-
Gear ratio	g_r	3.4 - 2.1 - 1.4 - 1.0 - 0.77	-

Simulations are done for the New European Driving Cycle (NEDC) [29], of which the vehicle speed is shown in Fig. 8. It consists of four identical urban cycles and one extra-urban cycle. For the electric power request, constant loads of 500, 1000, and 2000 W are used.

B. Strategies

The following strategies are implemented on simulation level and their results will be compared.

- *BL* Baseline strategy where the alternator power is equal to the requested load.
- *DP* This strategy solves the DP problem once for the complete driving cycle.
- *QP* This strategy solves the QP problem once for the complete driving cycle.
- *QP1* QP at each time step with adapted λ using (45), (52), and (48).
- *DP1* DP at each time step with adapted λ using (51) and (48).

The DP strategy is used with an input grid of 100 W and a state grid of 100 J. The DP1 strategy is used with an input grid of 10 W and does not need a state grid.

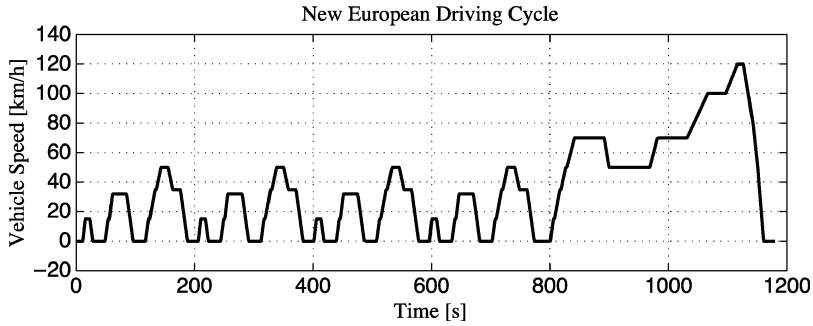

Fig. 8. New European Driving Cycle.

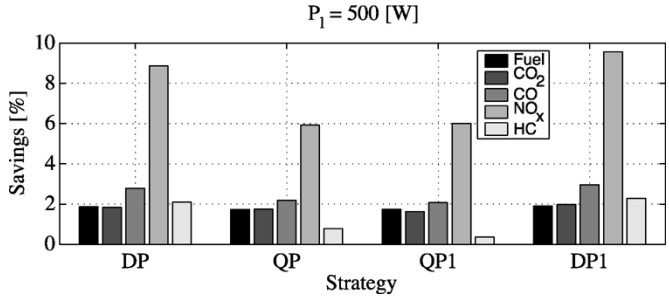

Fig. 9. Fuel and emissions reduction for $P_l = 500\,\mathrm{W}$.

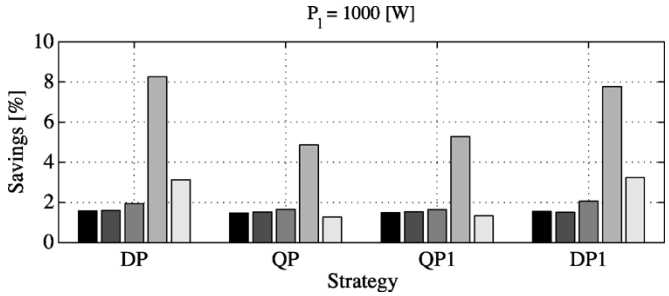

Fig. 10. Fuel and emissions reduction for $P_l = 1000\,\mathrm{W}$.

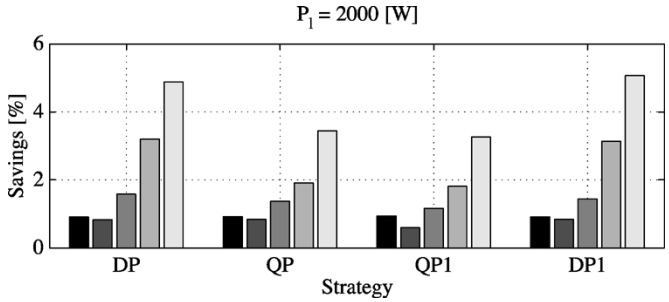

Fig. 11. Fuel and emissions reduction for $P_l = 2000\,\mathrm{W}$.

The PI controller (48) is tuned as follows. For λ_0 the value of the Lagrange multiplier resulting from the global QP optimization is used. The value depends on the electric load, a typical value is $\lambda_0 = 2.5$.

K_P and K_I are tuned such that for average values of $\varphi_1(t)$ and $\varphi_2(t)$, (49) becomes a critically damped second-order system with a bandwidth of 10^{-3} rad/s. The average values of $\varphi_1(t)$ and $\varphi_2(t)$ are

$$\tilde{\varphi}_1 = 2.5 \quad \text{and} \quad \tilde{\varphi}_2 = 2 \cdot 10^{-4}. \tag{56}$$

The corresponding values of K_P and K_I then become

$$K_P = 6.7 \cdot 10^{-7} \quad \text{and} \quad K_I = 3.3 \cdot 10^{-4}. \tag{57}$$

The QP1 and DP1 strategy do not guarantee that the endpoint constraint is satisfied. The difference in SOC is accounted for in the fuel consumption using the initial value of λ

$$fuel_c = \sum_{k=1}^{n} \mathrm{fuelrate}(k) - \lambda_0 \left(E_s(n) - E_s(0)\right). \tag{58}$$

C. Results

When the cost function represents only the fuel consumption, it turns out that for this case the CO_2, CO, and NO_x emissions are also reduced significantly. However, the emission of HC increases. Therefore, a weighted sum of fuel and HC emission is used as cost function. The weighting factors in (11) are $w_1 = w_5 = 1$ and $w_2 = w_3 = w_4 = 0$. This time, all emissions are reduced, at the cost of a slight decrease in fuel reduction. The savings with respect to the baseline strategy for the various loads are presented in Figs. 9, 10, and 11.

The resulting sequences of P_s for all strategies with $P_l = 1000$ W are shown in Fig. 12. The optimization anticipates on regenerative braking phases and generates less in between. The trajectories of P_e and P_m are shown in Fig. 13 and Fig. 14.

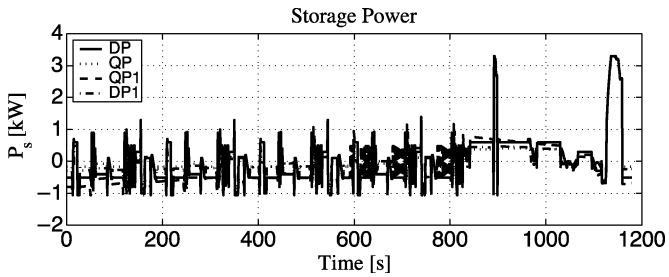

Fig. 12. Battery storage power.

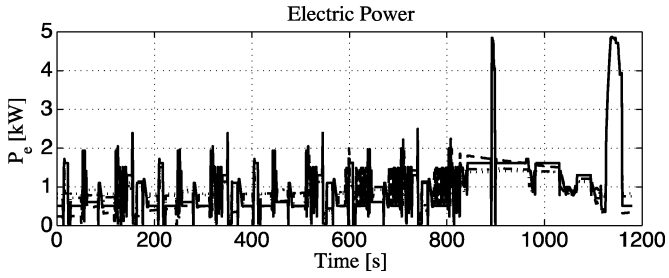

Fig. 13. Electrical power.

Fig. 15 shows the corresponding sequences of the SOC. The variation in SOC is small, because of the large capacity of the

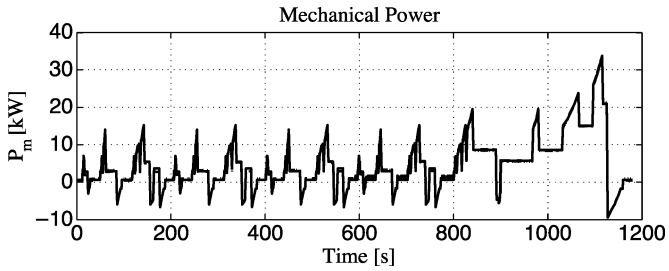

Fig. 14. Mechanical power.

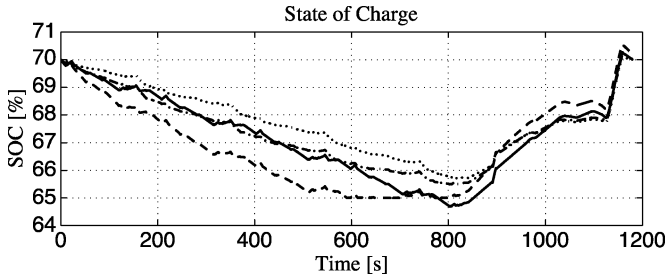

Fig. 15. Battery state of charge.

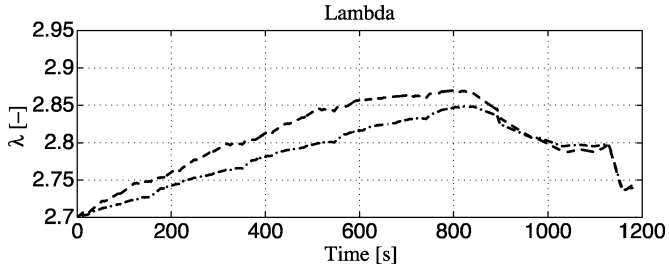

Fig. 16. Adaptive λ trajectory.

battery. This justifies that for this simulation, the battery efficiency is chosen independently of E_s.

The trajectories of the adaptive λ for the DP1 and QP1 strategies are shown in Fig. 16. The value of λ varies slightly around its initial value.

D. Evaluation

The simulations show that the strategies are working, as they all succeed in lowering the fuel consumption and the exhaust emissions. The results might be further improved by fine tuning the weighting factors of the cost function.

Most of the profit comes from regenerative braking, which delivers a certain amount of energy for free. As explained in [30], the baseline already exploits a part of the free energy from regenerative braking and that part increases with increasing load. Therefore the relative fuel savings of a strategy exploiting the full regenerative braking potential compared to the baseline are higher at low electric powers.

The adaptive strategies not using future knowledge perform equally well. For some loads, the DP1 strategy outscores the DP strategy, because of its finer input grid.

Both DP and QP do not find the global optimal solution of the nonlinear optimization problem. The DP algorithm uses the original nonlinear cost criterium, but restricts itself to a grid, whereas the QP algorithm finds the global optimum of a quadratic approximation of the original problem. The small difference between DP and QP for fuel use and CO_2 indicates that these terms in the nonlinear cost function are approximated accurately by a QP problem, and that the chosen grid is not too restrictive for the DP problem. For the other emissions, that show more nonsmooth behavior, the differences between DP and QP are larger, because the QP based methods use smooth convex approximations.

The DP1 strategy is the one to choose for, because of its good results and because it is easy implementable online.

Apart from regenerative braking, the strategies presented here benefit from differences in the incremental fuel rate at various operating points. For the fuel map used here, see Fig. 6, this variation in slope is rather small, which limits the additional fuel reduction that can be made with an energy management strategy on top of regenerative braking. The maps of the exhaust emissions show more variation, giving rise to higher reductions.

The performance is limited by the losses that occur during charging and discharging of the battery. As an alternative, an ultra capacitor can be used, which has a much higher efficiency, but also a lower capacity.

A detailed theoretical analysis on how the potential performance of energy management depends on the component characteristics is presented in [30]. It contains a comparison with results obtained with DP, which shows a reasonable correspondence with the analytic results.

VIII. Extension to a Parallel HEV

The strategies presented here can also be used for a mild HEV with an ISA that is directly connected to the engine. Examples are the Honda Insight [31], [32] and the Honda Civic IMA.

In such a vehicle, the engine and the ISA are always operating simultaneously and there is no freedom in the engine speed. The alternator power is still the only degree of freedom, but the operating range is larger, because the ISA can also work in propulsion mode, which means that P_e and P_g become negative.

Fuel reduction is then obtained mostly by the fact that a smaller engine can be used, because the ISA can be used for boosting to obtain a similar performance as a larger engine. A smaller engine has smaller friction and pumping losses, and thus a smaller drag torque, which results in less fuel consumption during propulsion, and also leaves more energy available for regenerative braking.

Full HEVs, such as the Toyota Prius [33], have both freedom in the engine speed and torque, and the engine and the electric motor can be operated independently. This gives more potential improvement but also makes the energy management problem more complex and requires some modifications to the strategies proposed here. The concept proposed here, using power-based models, making an online estimation of the optimal incremental costs, and using this for instantaneous optimization can still be applied.

IX. Conclusion

Several energy management strategies for the electrical power net are presented, that use either a prediction of the future or information about the current state of the vehicle,

to reduce the fuel consumption and exhaust emissions over a driving cycle.

Simulations show that the energy management concept is working. With the degree of freedom considered here and the component characteristics used, a fuel reduction of 2% can be obtained, while at the same time reducing the emissions. The largest part of the fuel reduction is obtained with regenerative braking.

The current approach does not require changes to the drive train and is therefore cheap to implement. The DP1 strategy is the most suitable for online implementation, as it exploits the non-convexity of the cost function and does not require a prediction of the future.

The strategies can also be applied to a mild HEV with an ISA. The approach can be extended for HEVs with more degrees of freedom.

REFERENCES

[1] J. G. Kassakian, H.-C. Wolf, J. M. Miller, and C. J. Hurton, "Automotive electrical systems circa 2005," *IEEE Spectrum*, vol. 33, no. 8, pp. 22–27, Aug. 1996.

[2] J. G. Kassakian, J. M. Miller, and N. Traub, "Automotive electronics power up," *IEEE Spectrum*, vol. 37, no. 5, pp. 34–39, May 2000.

[3] P. Nicastri and H. Huang, "42V PowerNet: providing the vehicle electrical power for the 21st century," in *Proc. SAE Future Transportation Technol. Conf.*, Costa Mesa, CA, Aug. 2000, SAE Paper 2000-01-3050.

[4] K. Ehlers, H. D. Hartmann, and E. Meissner, "42 V—An indication for changing requirements on the vehicle electrical system," *J. Power Sources*, vol. 95, pp. 43–57, 2001.

[5] A. Emadi, M. Ehsani, and J. M. Miller, *Vehicular Electric Power Systems: Land, Sea, Air, and Space Vehicles*. New York: Marcel Dekker, 2003.

[6] F. Liang, J. M. Miller, and X. Xu, "A vehicle electric power generation system with improved output power and efficiency," *IEEE Trans. Ind. Appl.*, vol. 35, no. 6, pp. 1341–1346, Nov.–Dec. 1999.

[7] J. S. Won and R. Langari, "Intelligent energy management agent for a parallel hybrid vehicle," in *Proc. Amer. Contr. Conf.*, Denver, CO, Jun. 2003.

[8] B. M. Baumann, G. Washington, B. C. Glenn, and G. Rizzoni, "Mechatronic design and control of hybrid electric vehicles," *IEEE/ASME Trans. Mechatronics*, vol. 5, no. 1, pp. 58–72, Mar. 2000.

[9] N. J. Schouten, M. A. Salman, and N. A. Kheir, "Fuzzy logic control for parallel hybrid vehicles," *IEEE Trans. Contr. Syst. Technol.*, vol. 10, no. 3, pp. 460–468, May 2002.

[10] E. D. Tate and S. P. Boyd, "Finding ultimate limits of performance for hybrid electric vehicles," in *Proc. SAE Future Transportation Technol. Conf.*, Costa Mesa, CA, Aug. 2000, SAE Paper 2000-01-3099.

[11] S. Delprat, J. Lauber, T. M. Guerra, and J. Rimaux, "Control of a parallel hybrid powertrain: optimal control," *IEEE Trans. Veh. Technol.*, vol. 53, no. 3, pp. 872–881, May 2004.

[12] M. Back, M. Simons, F. Kirschaum, and V. Krebs, "Predictive control of drivetrains," in *Proc. IFAC 15th Triennial World Congress*, Barcelona, Spain, 2002.

[13] C.-C. Lin, H. Peng, J. W. Grizzle, and J.-M. Kang, "Power management strategy for a parallel hybrid electric truck," *IEEE Trans. Contr. Syst. Technol.*, vol. 11, no. 6, pp. 839–849, Nov. 2003.

[14] T. Hofman and R. van Druten, "Energy analysis of hybrid vehicle powertrains," in *Proc. IEEE Int. Symp. Veh. Power Propulsion*, Paris, France, Oct. 2004.

[15] I. Arsie, M. Graziosi, C. Pianese, G. Rizzo, and M. Sorrentino, "Optimization of supervisory control strategy for parallel hybrid vehicle with provisional load estimate," in *Proc. 7th Int. Symp. Adv. Vehicle Control (AVEC)*, Arnhem, The Netherlands, Aug. 2004.

[16] V. H. Johnson, K. B. Wipke, and D. J. Rausen, "HEV control strategy for real-time optimization of fuel economy and emissions," in *Proc. Future Car Congress*, Washington, DC, Apr. 2000, SAE Paper 2000-01-1543.

[17] G. Paganelli, G. Ercole, A. Brahma, Y. Guezennec, and G. Rizzoni, "General supervisory control policy for the energy optimization of charge-sustaining hybrid electric vehicles," *JSAE Rev.*, vol. 22, no. 4, pp. 511–518, Apr. 2001.

[18] A. Sciarretta, L. Guzzella, and M. Back, "A real-time optimal control strategy for parallel hybrid vehicles with on-board estimation of the control parameters," in *Proc. IFAC Symp. Adv. Automotive Contr.*, Salerno, Italy, Apr. 19–23, 2004.

[19] I. Kolmanovsky, I. Siverguina, and B. Lygoe, "Optimization of powertrain operating policy for feasibility assessment and calibration: stochastic dynamic programming approach," in *Proc. Amer. Contr. Conf.*, vol. 2, Anchorage, AK, May 2002, pp. 1425–1430.

[20] C.-C. Lin, H. Peng, and J. W. Grizzle, "A stochastic control strategy for hybrid electric vehicles," in *Proc. Amer. Contr. Conf.*, Boston, MI, Jun. 2004, pp. 4710–4715.

[21] B. de Jager, "Predictive storage control for a class of power conversion systems," in *Proc. Europ. Contr. Conf.*, Cambridge, UK, Sep. 2003.

[22] E. Nuijten, M. Koot, J. Kessels, B. de Jager, M. Heemels, W. Hendrix, and P. van den Bosch, "Advanced energy management strategies for vehicle power nets," in *Proc. EAEC 9th Int. Congress: Europ. Automotive Industry Driving Global Changes*, Paris, France, Jun. 2003.

[23] M. Koot, J. Kessels, B. de Jager, M. Heemels, and P. van den Bosch, "Energy management strategies for vehicle power nets," in *Proc. Amer. Contr. Conf.*, Boston, MA, Jun. 2004, pp. 4072–4077.

[24] D. P. Bertsekas, *Dynamic Programming and Optimal Control*. Belmont, MA: Athena Scientific, 1995.

[25] R. Fletcher, *Practical Methods of Optimization*, 2nd ed. New York: Wiley, 2000.

[26] J. M. Maciejowski, *Predictive Control With Constraints*. Englewood Cliffs, NJ: Prentice-Hall, 2001.

[27] P. P. J. van den Bosch and F. A. Lootsma, "Scheduling of power generation via large-scale nonlinear optimization," *J. Optimiz. Theory Appl.*, vol. 55, pp. 313–326, 1987.

[28] M. J. West, C. M. Bingham, and N. Schofield, "Predictive control for energy management in all/more electric vehicles with multiple energy storage units," in *Proc. IEEE Int. Electric Machines and Drives Conf.*, vol. 1, Jun. 2003, pp. 222–228.

[29] NEDC, European Council Directive, 70/220/EEC with amendments.

[30] M. Koot, J. Kessels, B. de Jager, and P. van den Bosch, "Energy management for vehicle power nets," in *Proc. FISITA World Automotive Conf.*, Barcelona, Spain, May 2004.

[31] K. Fukuo, A. Fujimura, M. Saito, K. Tsunoda, and S. Takiguchi, "Development of the ultra-low-fuel-consumption hybrid car—insight," *JSAE Rev.*, vol. 22, no. 1, pp. 95–103, Jan. 2001.

[32] K. J. Kelly, M. Zolot, G. Glinsky, and A. Hieronymus, Test results and modeling of the Honda insight using ADVISOR, 2001.

[33] D. Hermance and S. Sasaki, "Hybrid electric vehicles take to the streets," *IEEE Spectrum*, vol. 35, no. 11, pp. 48–52, Nov. 1998.

Michiel Koot was born in Sittard, The Netherlands, in 1977. He received the M.Sc. degree in mechanical engineering from the Technische Universiteit Eindhoven, Eindhoven, The Netherlands, in 2001.

Currently, he is a Ph.D. student with the Dynamics and Control Technology Group, Department of Mechanical Engineering, Technische Universiteit Eindhoven. His research interests include control of mechanical systems, optimization, and energy management for automotive vehicles.

J. T. B. A. (John) Kessels (S'04) received the B.Sc degree (with honors) in electrical engineering from Fontys Hogescholen, Eindhoven, The Netherlands, in 2000, and the M.Sc. degree (*cum laude*) in electrical engineering from the Technische Universiteit Eindhoven, The Netherlands, in 2003.

Currently, he is a Ph.D. student with the Department of Electrical Engineering, Section Control Systems, Technische Universiteit Eindhoven. His research interests are modeling and control of the electric power supply system in vehicles.

Bram de Jager received the M.Sc. degree in mechanical engineering from Delft University of Technology, Delft, The Netherlands, and the Ph.D. degree from the Technische Universiteit Eindhoven, The Netherlands.

He was with the Delft University of Technology and Stork Boilers BV, Hengelo, The Netherlands. Currently, he is with the Technische Universiteit Eindhoven. His research interests include robust control of (nonlinear) mechanical systems, integrated control and structural design, control of fluidic systems, control structure design, and application of symbolic computation in nonlinear control.

W. P. M. H. (Maurice) Heemels was born in St. Odiliënberg, The Netherlands, in 1972. He received the M.Sc. degree (with honors) from the Department of Mathematics and the Ph.D. degree (*cum laude*) from the Department of Electrical Engineering of the Technische Universiteit Eindhoven, The Netherlands, in 1995 and 1999, respectively. He was awarded the ASML prize for the best Ph.D. thesis of the Technische Universiteit Eindhoven in 1999/2000 in the area of fundamental research.

From 2000 to 2004 he has been an Assistant Professor with the Control Systems Group, Department of Electrical Engineering, Technische Universiteit Eindhoven. In June 2004, he moved to the Embedded Systems Institute, Eindhoven, The Netherlands, where he is working as a research fellow. He spent three months as a visiting professor with the ETH in Zürich, Switzerland, in 2001 and a same period with the company Océ in Venlo, The Netherlands, in 2004. His research interests include modeling, analysis, and control of hybrid and nonsmooth systems and their applications to industrial design problems for embedded systems.

P. P. J. (Paul) van den Bosch (M'84) received the M.Sc. degree (*cum laude*) in electrical engineering and the Ph.D. degree in optimization of electric energy systems from Delft University of Technology, The Netherlands.

After his study, he joined the Control Systems Group, Delft University of Technology, and was appointed full professor in control engineering in 1988. In 1993, he was appointed full professor in the Control Systems Group of Electrical Engineering at the Technische Universiteit Eindhoven and in 2004, a part-time professor with the Department of Biomedical Engineering. His research interests concern modeling, optimization, and control of dynamical systems. In his career, he has created many common research projects with industry, among others automotive applications, large-scale electric systems, advanced electromechanical actuators, and recently, embedded systems and biomedical modeling. Beside his scientific activities, he has received several prizes for his educational activities and several patents.

Dr. van den Bosch has served on boards of journals (Journal A) and conference committees.

Maarten Steinbuch (S'83–M'89–SM'02) received the M.Sc. degree (*cum laude*) in mechanical engineering and the Ph.D. degree in modeling and control of wind energy conversion systems from Delft University of Technology, Delft, The Netherlands, in 1984 and 1989, respectively.

He is currently a Full Professor with the Department of Mechanical Engineering, Technische Universiteit Eindhoven, Eindhoven, The Netherlands. From 1984 to 1987, he was a Research Assistant with Delft University of Technology and KEMA (Power Industry Research Institute), Arnhem, The Netherlands. From 1987 to 1998, he was with Philips Research Laboratories, Eindhoven, as a Member of the Scientific Staff, working on modeling and control of mechatronic applications. From 1998 to 1999, he was a Manager of the Dynamics and Control Group, Philips Center for Manufacturing Technology. His research interests are modeling and control of motion systems.

Dr. Steinbuch was an Associate Editor of the IEEE TRANSACTIONS ON CONTROL SYSTEMS TECHNOLOGY from 1993 to 1997, of IFAC Control Engineering Practice from 1994 to 1996, and of the IEEE *Control Systems Magazine* from 1999 to 2002. He is currently Editor-at-Large of the *European Journal of Control*. In 2003, he received the Best Teacher 2002/2003 award from the Department of Mechanical Engineering, Technische Universiteit Eindhoven.